This is the accepted manuscript made available via CHORUS. The article has been published as:

Anisotropy-induced spin parity effects

Shuntaro Sumita, Akihiro Tanaka, and Yusuke Kato

Phys. Rev. B **110**, L100403 — Published 6 September 2024

DOI: 10.1103/PhysRevB.110.L100403

Anisotropy-Induced Spin Parity Effects

Shuntaro Sumita,[1,2,3,*] Akihiro Tanaka,[4] and Yusuke Kato[1,5]

[1]*Department of Basic Science, The University of Tokyo, Meguro, Tokyo 153-8902, Japan*
[2]*Komaba Institute for Science, The University of Tokyo, Meguro, Tokyo 153-8902, Japan*
[3]*Condensed Matter Theory Laboratory, RIKEN CPR, Wako, Saitama 351-0198, Japan*
[4]*Research Center for Materials Nanoarchitectonics, National Institute for Materials Science, Tsukuba, Ibaraki 305-0044, Japan*
[5]*Quantum Research Center for Chirality, Institute for Molecular Science, Okazaki, Aichi 444-8585, Japan*

(Dated: August 2, 2024)

Spin parity effects refer to those special situations where a dichotomy in the physical behavior of a system arises, solely depending on whether the relevant spin quantum number is integral or half-odd integral. As is the case with the Haldane conjecture in antiferromagnetic spin chains, their pursuit often derives deep insights and invokes new developments in quantum condensed matter physics. Here we put forth a simple and general scheme for generating such effects in any spatial dimension through the use of anisotropic interactions, and a setup within reasonable reach of state-of-the-art cold-atom implementations. We demonstrate its utility through a detailed analysis of the magnetization behavior of a specific one-dimensional spin chain model—an anisotropic antiferromagnet in a transverse magnetic field, unraveling along the way the quantum origin of finite-size effects observed in the magnetization curve that had previously been noted but not clearly understood.

Introduction.—It often happens that a pivotal development in quantum magnetism is triggered by the discovery of a *spin parity effect* (SPE)— a phenomenon in which the behavior of a magnetic system sharply depends on the *parity of twice the spin quantum number* S. The Haldane conjecture on antiferromagnetic spin chains [1–3], the prime example of an SPE, asserts that a spectral gap exists between the ground state (GS) and excited states for integer S, whereas the corresponding spectrum is gapless for half-odd-integer S. While this claim is now long established, the activity that ensued has since evolved into themes central to present day condensed matter physics. An example with far-reaching consequences to quantum many-body systems, is the no-go theorem of Lieb, Schultz, and Mattis (LSM), which in its original form prohibits the existence of a unique and featureless gapped GS in an $S = 1/2$ Heisenberg chain [4]. Among its extensions are those to: general S [5–12], higher dimensions [13–23], various symmetries [19–22, 24–28], and electron systems [24–26, 29]. The quantum dynamics of solitons [30–32] and skyrmions [33] in chiral magnets hosting Dzyaloshinskii–Moriya interactions, is another active research front where SPEs have recently been identified; there the soliton/skyrmion states were found to have spin-parity-dependent crystal momenta.

Given how SPEs continue to shed new light on quantum condensed matter, it is desirable to have a generic and comprehensive scheme with which to generate them. It is the purpose of this Letter is to put forth just such a method. Our approach incorporates *anisotropic interactions* as its key element and works in any spatial dimension, which is to be compared with how SPEs—including those mentioned above usually have dimension-specific origins. We are also motivated by rapid theoretical [34] and experimental [35, 36] progress in cold-atom physics that have come a long way toward implementing higher-S quantum spin systems with strong anisotropy.

To best illustrate our strategy, we apply it to a one-dimensional (1D) quantum spin system which has the merit of 1) being amenable to detailed analysis and 2) exhibiting a clear SPE that manifests itself in raw finite-size numerical data. Feasibility aside, this problem turns out to be interesting in its own rights: the finite-size effect studied, while long-known has a topological significance (in the sense of Haldane [37]) that had gone unnoticed. The anisotropy-induced SPE in this model is nontrivial in that it evades detection by LSM-type arguments. Finally it can be considered an immediate target for cold-atom implementations. Generalizations to a far-wider range of quantum magnets will be discussed afterwards.

Model and exact diagonalization.—The Hamiltonian of our choice is

$$\hat{\mathcal{H}} = J \sum_{j=1}^{L} \hat{\boldsymbol{S}}_j \cdot \hat{\boldsymbol{S}}_{j+1} - H \sum_{j=1}^{L} \hat{S}^z_j + K \sum_{j=1}^{L} (\hat{S}^y_j)^2. \tag{1}$$

The $J(>0)$ and H terms are the exchange and Zeeman interactions, respectively, while the $K(\geq 0)$ term is an easy-plane single-ion anisotropy. L stands for the number of sites. We impose a periodic boundary condition, with the system always consisting of an even number of sites.

We display in the first two rows of Fig. 1 how the GS expectation value of the magnetization, $m_z := \frac{1}{L}\sum_{j=1}^{L} \langle \hat{S}^z_j \rangle_{\mathrm{GS}}$ evolves as a function of H. Here J is set to unity. The numerical exact diagonalization was performed for various values of S with the use of QuSpin [38–40]. Numerics for other parameter choices are given in the Supplemental Materials (SM) [41]. The jumps in the magnetization are due to level crossings (LCs) between the GS and the first excited state; such features had been noted [63–66] but not fully understood. We find that they are accompanied by the alternation in the GS's crystal momentum between two values, 0 (violet) and π (green). Furthermore, a marked difference in behavior was found depending on the magnitude of K. This is summarized in the table below, where we indicate by N_{c} the number of

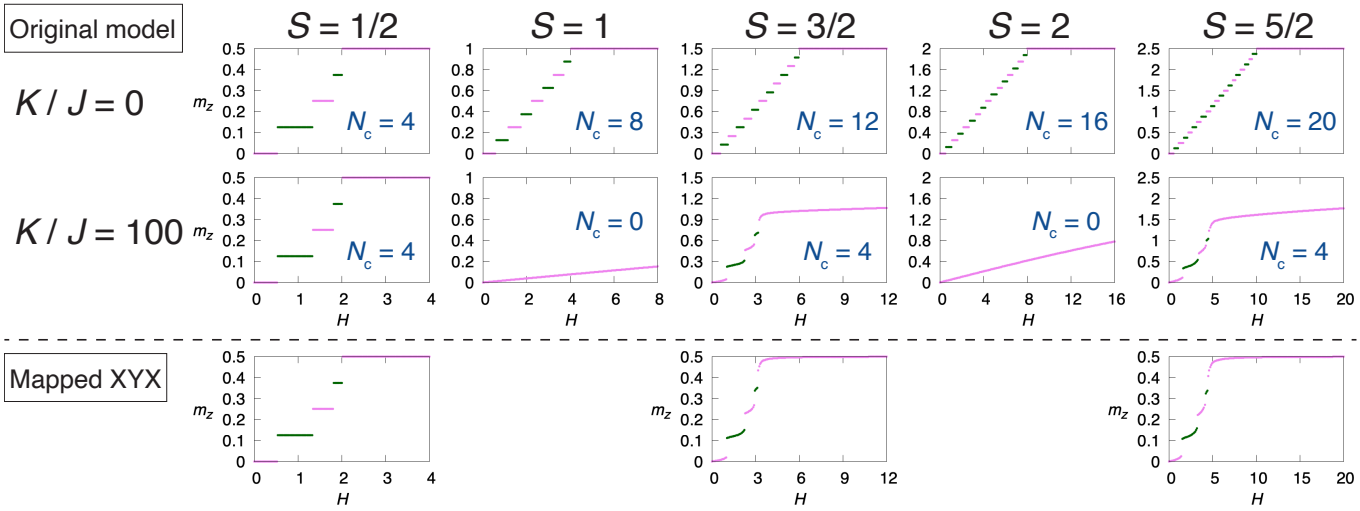


FIG. 1. Magnetization m_z vs magnetic field H curves obtained by numerical calculations. L is set to 8 for all panels. The violet and green lines represent that the GS has crystal momenta 0 and π, respectively. (Top and middle panels) Results for zero and large anisotropy in the original model. (Bottom panels) Results in the XYX model that is obtained by the mapping for large K and half-odd-integer spins.

LCs:

N_c	odd $2S$	even $2S$
$K = 0$, small K	LS	LS
$K \gg J$	$L/2$	0

(2)

When K is small or zero the jumps are present irrespective of the spin parity, while in the strongly anisotropic regime $K \gg J$ they manifest themselves only when S is a half-odd integer. We discuss the two cases in turn.

$K = 0$: *XX model and Tomonaga–Luttinger liquid (TLL).*— Our objective here is to explain the LCs with $N_c = LS$ between the 0- and π-momentum states for $K = 0$ (top panels in Fig. 1). Before dealing with the full model Eq. (1), it is instructive to warm up with the spin-1/2 XX model: $\hat{\mathcal{H}}_{XX} = J\sum_{j=1}^{L}(\hat{S}_j^x\hat{S}_{j+1}^x + \hat{S}_j^y\hat{S}_{j+1}^y) - H\sum_{j=1}^{L}\hat{S}_j^z$, which allows for an intuitive understanding of the momentum switching. The Jordan–Wigner (JW) transformation [67] maps this model into a non-interacting spinless fermion:

$$\hat{\mathcal{H}}_{XX} = \sum_{l=1}^{L}(J\cos k_l - H)\hat{a}_{k_l}^\dagger\hat{a}_{k_l} + \frac{LH}{2}, \tag{3}$$

where $\hat{a}_{k_l}$ is the annihilation operator of the JW fermion carrying momentum k_l. The Hamiltonian commutes with the fermion number operator $\hat{N}_a := \sum_{l=1}^{L}\hat{a}_{k_l}^\dagger\hat{a}_{k_l}$, where the sum is taken over $k_l = (2l-1)\pi/L$ when N_a is even, while $k_l = 2(l-1)\pi/L$ for odd N_a. Block-diagonalizing $\hat{\mathcal{H}}_{XX}$ within eigensectors of $\hat{N}_a$, we show in Fig. 2(a) the energy eigenvalues $E_{N_a}(H)$ as a function of H, where plots for even (odd) N_a are colored in violet (green). As the magnetic field H is ramped up the GS eigenvalue of $\hat{N}_a$ increases by unit increments which translates back to the number of up spins in the original model: $\hat{N}_a = \hat{S}_{\rm tot}^z + L/2$, where $\hat{S}_{\rm tot}^z = \sum_{j=1}^{L}\hat{S}_j^z$.

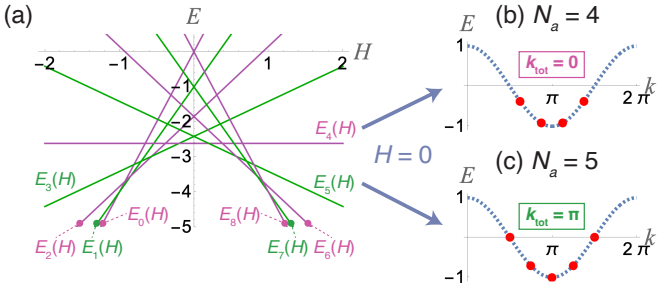


FIG. 2. (a) Energy eigenvalues of the spin-1/2 XX chain with $L = 8$ for each $\hat{N}_a$ sector. Momentum–energy relations for $H = 0$ in the sectors with $N_a = 4$ and 5 are shown in (b) and (c), respectively.

We depict the cosine term in Eq. (3) for $N_a = 4$ and 5 in Figs. 2(b) and 2(c), respectively. Clearly the total momentum $k_{\rm tot} := \left\langle\sum_{l=1}^{L} k_l\hat{a}_{k_l}^\dagger\hat{a}_{k_l}\right\rangle \pmod{2\pi}$ is zero for even N_a, and π for odd N_a. Returning now to the Heisenberg model Eq. (1) with $K = 0$, this momentum-counting argument no longer applies as the $\sum_{j=1}^{L} J\hat{S}_j^z\hat{S}_{j+1}^z$ term generates interactions between the JW fermions. Using the Bethe ansatz, however, the total momentum $k_{\rm tot}$ can be shown to remain unaffected, despite the phase shift each momentum k_l receives from particle scattering [41, 68]. Whether the GS momentum is 0 or π is thus determined solely by the parity of the number of up spins.

The preceding argument was limited to $S = 1/2$. To generalize to arbitrary spin, we incorporate the powerful machinery of the TLL theory, known to correctly capture (for higher S cases as well) the behavior of the gapless, linear dispersion of the $K = 0$ model, i.e., the Heisenberg model under an applied magnetic field. In this framework, a low-energy excited state is fully characterized by a quartet of integer-valued quantum numbers: ΔN (charge excitation), ΔD (current excitation), and

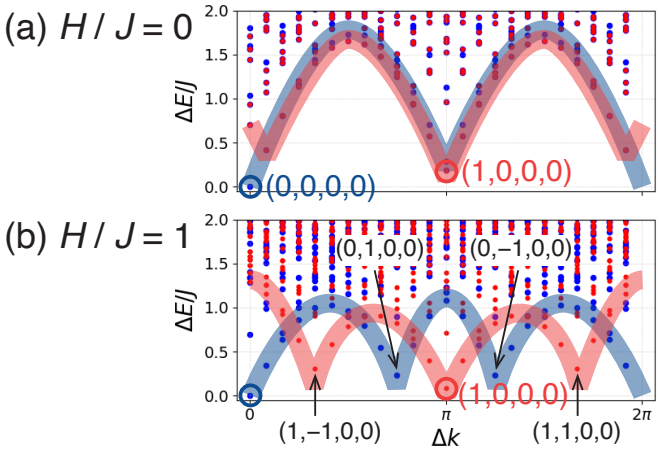


FIG. 3. Energy dispersions of the spin-1/2 Heisenberg chain with $L = 24$ for (a) $H/J = 0$ and (b) 1. In both panels, the GS is positioned at $(\Delta E, \Delta k) = (0, 0)$, and the other points show the spectrum of excited states. Each blue (red) point represents the spectrum in the $\Delta S^z_{\rm tot} = \Delta N = 0$ (1) sector. Sets of quantum numbers $(\Delta N, \Delta D, N^+, N^-)$ are shown for some characteristic points. The translucent lines are guides for the eyes.

$N^\pm$ (right/left-moving particle-hole pair). The corresponding energy eigenvalue and momentum are given by [69]

$$\Delta E = \frac{2\pi v}{L}\left[\frac{(\Delta N)^2}{4K_{\rm L}} + K_{\rm L}(\Delta D)^2 + N^+ + N^-\right] + \mu\Delta N, \quad (4)$$

$$\Delta k = 2\pi\rho\Delta D + \frac{2\pi}{L}[\Delta N\Delta D + N^+ - N^-] + \pi\Delta N, \quad (5)$$

where $K_{\rm L}$, v, μ, and $2\pi\rho$ are each the Luttinger liquid parameter, the excitation's velocity, the chemical potential, and the intrinsic momentum [70, 71]. The last term in Eq. (5) arises from antiferromagnetic correlations inherent to our lattice model; retaining it on taking the continuum limit is crucial. The only quantum number coupling to a magnetic field is ΔN; it then follows that the state $(\Delta N, \Delta D, N^+, N^-) = (1, 0, 0, 0)$, which amounts to a change in momenta by $\Delta k = \pi$, always becomes the next GS as the field is increased. The quantity $\langle \hat{S}^z_{\rm tot}\rangle_{\rm GS}$, which is conserved when $K = 0$, increases by one each time a crossover with $\Delta N = 1$ takes place. Accordingly the value of $\langle \hat{S}^z_{\rm tot}\rangle_{\rm GS}$ undergoes the sequence: $0 \to 1 \to \cdots \to LS$. This is in agreement with the relation $N_{\rm c} = LS$ [Eq. (2)], which we extracted from the magnetization processes in the top panels of Fig. 1.

Figures 3(a) and 3(b) show in full detail the energy dispersions of the spin-1/2 Heisenberg model, which we use to check the validity of the above picture. States for which $\Delta S^z_{\rm tot} := \langle \hat{S}^z_{\rm tot}\rangle - \langle \hat{S}^z_{\rm tot}\rangle_{\rm GS}$ $(= \Delta N)$ is 0 and 1 are each plotted as blue and red points. The low-energy spectrum contains conformal towers, located at $k = 0, \pm 2\pi\rho$ for $\Delta S^z_{\rm tot} = 0$ (blue lines), and at $k = \pi, \pi \pm (2\pi\rho + 2\pi/L)$ for $\Delta S^z_{\rm tot} = 1$ (red lines). The results are consistent with Eqs. (4) and (5); in particular, ρ is equal to 1/2 for the "half-filling" case $H = 0$ [cf. Fig. 2(b)].

$\mathbb{Z}_2$ symmetry and crystal momentum.—We proceed to nonzero K cases, where $\hat{S}^z_{\rm tot}$ is not conserved. We can still take advantage of a discrete $\mathbb{Z}_2 \times \mathbb{Z}_2^T$ symmetry of the Hamiltonian of Eq. (1), where the unitary part is generated by $\hat{Z} := \bigotimes_{j=1}^{L} e^{i\pi(S-\hat{S}^z_j)}$, i.e., a π-rotation of all spins with respect to the z axis. Noting that $\hat{Z}^2 = 1$ for any S, the Hamiltonian can be block-diagonalized into sectors labeled by the $\mathbb{Z}_2$ values $\hat{Z} = \pm 1$: $\hat{\mathcal{H}} = \hat{\mathcal{H}}^{(+)} \oplus \hat{\mathcal{H}}^{(-)}$. The following is true for arbitrary positive values of K:

Theorem 1. *When the GS of the Hamiltonian Eq. (1) is a simultaneous eigenstate with $\hat{Z} = +1$ (-1), it has a crystal momentum 0 (π).*

A sketch of the proof goes as follows; the full details are given in the SM [41]. Let $|\boldsymbol{m}\rangle := |m_1 m_2 \ldots m_L\rangle$ $(m_j = -S, -S+1, \ldots, S)$ be the usual spin basis such that $\hat{S}^z_j |\boldsymbol{m}\rangle = m_j |\boldsymbol{m}\rangle$. Introducing a *signed basis* $|\widetilde{\boldsymbol{m}}\rangle := (-1)^{\delta(\boldsymbol{m})} |\boldsymbol{m}\rangle$ with $\delta(\boldsymbol{m}) := \sum_{j=1}^{L} j(S - m_j)$, one can show that (i) off-diagonal elements of the Hamiltonian are nonpositive, and (ii) both eigensectors with $\hat{Z} = \pm 1$ are irreducible. From (i) and (ii), the Perron–Frobenius theorem [72, 73] applied to the Hamiltonian block $\hat{\mathcal{H}}^{(\pm)}$ leads to the uniqueness of the GS in each eigensector given by $\left|\Psi^{(\pm)}_{\rm GS}\right\rangle = \sum_{\boldsymbol{m}\in V^{(\pm)}} a(\boldsymbol{m}) |\widetilde{\boldsymbol{m}}\rangle$, where $a(\boldsymbol{m}) > 0$ and $V^{(\pm)} := \left\{\boldsymbol{m} \,\middle|\, \hat{Z}|\widetilde{\boldsymbol{m}}\rangle = \pm|\widetilde{\boldsymbol{m}}\rangle\right\}$. Further, the one-site translation operator $\hat{T}$ affects the sign of the basis: $(-1)^{\delta(\hat{T}(\boldsymbol{m}))} = (-1)^{\sum_j (S-m_j)}(-1)^{\delta(\boldsymbol{m})} = \hat{Z}(-1)^{\delta(\boldsymbol{m})}$. Combining these, a little algebra shows that $\hat{T}\left|\Psi^{(\pm)}_{\rm GS}\right\rangle = \pm\left|\Psi^{(\pm)}_{\rm GS}\right\rangle$.

Theorem 1 implies that the LCs between 0- and π-momentum states are characterized by the parity switching of $\hat{S}^z_{\rm tot}$, although $\hat{S}^z_{\rm tot}$ itself is in general not conserved. Moreover, as long as $\hat{Z}$ is preserved, the LCs can survive even when the translation symmetry is broken.

Large K: perturbation theory.—We now address the SPE arising at large K (middle panels in Fig. 1). This can be understood in terms of a perturbation theory applicable for $K \gg J, H$. The non-perturbative Hamiltonian is just $\hat{\mathcal{H}}_0 = K\sum_{j=1}^{L}(\hat{S}^y_j)^2$, which reduces to a single-site problem: remembering that K is positive, the GS of $\hat{\mathcal{H}}_0$ is just a product state of doublets $|S^y_j = \pm\frac{1}{2}\rangle$ residing on each site when S is a half-odd integer. Meanwhile a unique GS $|S^y_j = 0\rangle$ is formed for integer S (Fig. 4). Since the magnitude of the energy gap from the GS is of order $O(K)$, excited states are negligible in discussing the large-K physics. In other words, at low energies our model in the large-K limit translates into effective spin-0 and spin-1/2 systems for integer and half-odd-integer S cases, respectively [74]. In the former case, the GS is unique and trivial even when the perturbation $\hat{\mathcal{H}} - \hat{\mathcal{H}}_0$ is switched on, as long as $K \gg J, H$ is satisfied, explaining the absence of LCs. This GS can be identified with the so-called large-D phase, a gapped phase known to be topologically trivial [75–79].

The situation is quite different in half-odd-integer spin cases owing to the GS degeneracy of the non-perturbative Hamiltonian. Working within a first-order perturbation scheme, we

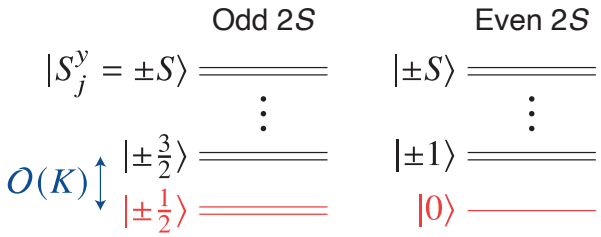


FIG. 4. Energy levels of the K model on the jth site. The GS degeneracy is two (one) in odd-$2S$ (even-$2S$) systems.

derive the following effective spin-1/2 XYX model:

$$\hat{\mathcal{H}}_{\rm map} = \widetilde{J}\sum_{j=1}^{L}(\hat{s}_j^x\hat{s}_{j+1}^x + \Delta\hat{s}_j^y\hat{s}_{j+1}^y + \hat{s}_j^z\hat{s}_{j+1}^z) - \widetilde{H}\sum_{j=1}^{L}\hat{s}_j^z, \quad (6)$$

where $\hat{\boldsymbol{s}}_j$ is the effective spin-1/2 operator on the jth site; see the SM for derivations [41]. The coefficients are defined as $\widetilde{J} := J/\Delta$, $\widetilde{H} := H/\sqrt{\Delta}$ with $\Delta := (S+1/2)^{-2}$. Notice that the single-ion anisotropy of the original Hamiltonian has effectively transformed here into an anisotropy of the exchange interaction. Numerical calculations for $\hat{\mathcal{H}}_{\rm map}$ are shown in the bottom panels of Fig. 1, where we find a good agreement between the obtained magnetization curve in the low-field regime with those of the original model (middle panels of Fig. 1). This reduction to effective spin-1/2 systems naturally explains the entry $N_{\rm c} = L/2$ in Eq. (2).

Generalization to higher dimensions and implementation.— Crucially one notices that anisotropy-induced SPEs are *not* specific to our model, Eq. (1): in the presence of a dominant K-term, the spectrum *always* reduces to Fig. 4 in the large-K limit, whatever the spatial dimension D, the lattice geometry, or the Hamiltonian itself are. Our perturbative scheme applies therefore to a much wider variety of spin systems.

Consider how this works for nearest-neighbor Heisenberg models on D-dimensional hypercubic lattices in the absence of external fields. As in $D = 1$, the spectral gap $\sim O(K)$ remains robust for integer spins, while the low energy physics of the half-integer spin systems are represented by effective spin-1/2 XYX models. The latter spontaneously breaks the spin rotation symmetry around the y axis, accompanied by a gapless Nambu–Goldstone mode.

Though new features arise, this SPE persists when terms which disrupt spin ordering (e.g., frustrated exchange and four-body interactions) are added. A trivially gapped state continues to form for integer spins, whereas the effective spin-1/2 model for the half-odd-integer spin case can now also sustain a degenerate spin-Peierls state [80–84] as well as a topologically ordered phase (see the SM for digressions [41]). Somewhat surprisingly, this dichotomy arises even under conditions where the LSM theorem [4–29] predicts no SPE. *The foregoing discussion on Eq. (1), a 1D model with only an on-site $\mathbb{Z}_2 \times \mathbb{Z}_2^T$ symmetry, in fact serves as an example of this highly nontrivial case.* A dominant K-term thus constitutes a simple but powerful point of departure for creating SPEs.

Finally we comment on the implications for experiments. Higher-S systems of finite size are becoming accessible with recent cold atom technologies. Indeed the 1D Hamiltonian Eq. (1), at least for $S = 1$, has recently been implemented in ultracold ^{87}Rb atoms in an optical lattice, where the single-ion anisotropy is controllable [35, 36]. Although ferromagnetic correlations were realized in these experiments, it is possible to make them antiferromagnetic by using negative temperature states [85, 86]. There are also reasons to anticipate the relevance of our approach to magnetic materials as well. Notably, our numerical results show that SPEs persist even when K and J are of the same order (see Fig. S1 in SM [41]), a regime better suited for materials search. Moreover, we expect traces of the SPE to be detectable in the thermodynamic limit, to which actual materials correspond: half-odd-integer spin systems would exhibit a small hysteresis in the magnetization curve due to the dense LCs, as observed in a classical chiral magnet [87]. This is not the case with integer spin systems.

Summary.—We analyzed an antiferromagnetic spin chain with easy-plane anisotropy, focusing on LCs between states with momenta 0 and π which alternately appear as a transverse magnetic field is increased. At zero or small anisotropy the LCs were accounted for using TLL theory and exact symmetry arguments. At strong anisotropy the LCs occur only for half-odd-integer spins. We showed how the latter is a realization of a very generic anisotropy-induced SPE, whose implementation is likely within reach of cold-atom technologies and magnetic materials science.

The authors are grateful to Sohei Kodama for earlier collaboration on related topics, and Shunsuke C. Furuya, Akira Furusaki, and Masaya Kunimi for informative discussions. This work was supported by JSPS KAKENHI Grants No. JP23K13056, No. JP23K03333, No. JP20K03855, No. JP21H01032, and No. JP19K03662, and JST CREST Grant No. JPMJCR19T2. The computation in this work was done using the facilities of the Supercomputer Center, the Institute for Solid State Physics, the University of Tokyo.

* s-sumita@g.ecc.u-tokyo.ac.jp

[1] F. D. M. Haldane, Ground State Properties of Antiferromagnetic Chains with Unrestricted Spin: Integer Spin Chains as Realisations of the O(3) Non-Linear Sigma Model, arXiv:1612.00076.
[2] F. D. M. Haldane, Continuum dynamics of the 1-D Heisenberg antiferromagnet: Identification with the O(3) nonlinear sigma model, Phys. Lett. A **93**, 464 (1983).
[3] F. D. M. Haldane, Nobel Lecture: Topological quantum matter, Rev. Mod. Phys. **89**, 040502 (2017).
[4] E. Lieb, T. Schultz, and D. Mattis, Two soluble models of an antiferromagnetic chain, Ann. Phys. **16**, 407 (1961).
[5] M. Kolb, Symmetry and boundary condition of planar spin systems, Phys. Rev. B **31**, 7494 (1985).
[6] I. Affleck and E. H. Lieb, A proof of part of Haldane's conjecture on spin chains, Lett. Math. Phys. **12**, 57 (1986).
[7] M. Oshikawa, M. Yamanaka, and I. Affleck, Magnetization Plateaus in Spin Chains: "Haldane Gap" for Half-Integer Spins,

Phys. Rev. Lett. **78**, 1984 (1997).
[8] M. Yamanaka, M. Oshikawa, and I. Affleck, Nonperturbative Approach to Luttinger's Theorem in One Dimension, Phys. Rev. Lett. **79**, 1110 (1997).
[9] T. Koma, Spectral Gaps of Quantum Hall Systems with Interactions, J. Stat. Phys. **99**, 313 (2000).
[10] H. Tasaki, Lieb–Schultz–Mattis Theorem with a Local Twist for General One-Dimensional Quantum Systems, J. Stat. Phys. **170**, 653–671 (2018).
[11] H. Tasaki, The Lieb–Schultz–Mattis theorem. A topological point of view, in *The Physics and Mathematics of Elliott Lieb*, Vol. 2, edited by R. L. Frank, A. Laptev, M. Lewin, and R. Seiringer (European Mathematical Society Press, 2022) pp. 405–446.
[12] Y. Ogata, Y. Tachikawa, and H. Tasaki, General Lieb–Schultz–Mattis Type Theorems for Quantum Spin Chains, Commun. Math. Phys. **385**, 79 (2021).
[13] M. Oshikawa, Commensurability, Excitation Gap, and Topology in Quantum Many-Particle Systems on a Periodic Lattice, Phys. Rev. Lett. **84**, 1535 (2000).
[14] M. B. Hastings, Lieb-Schultz-Mattis in higher dimensions, Phys. Rev. B **69**, 104431 (2004).
[15] M. B. Hastings, Sufficient conditions for topological order in insulators, Europhys. Lett. **70**, 824 (2005).
[16] M. B. Hastings, Locality in Quantum Systems, arXiv:1008.5137.
[17] B. Nachtergaele and R. Sims, A Multi-Dimensional Lieb-Schultz-Mattis Theorem, Commun. Math. Phys. **276**, 437 (2007).
[18] S. Bachmann, A. Bols, W. De Roeck, and M. Fraas, A Many-Body Index for Quantum Charge Transport, Commun. Math. Phys. **375**, 1249–1272 (2019).
[19] Y. Yao and M. Oshikawa, Generalized Boundary Condition Applied to Lieb-Schultz-Mattis-Type Ingappabilities and Many-Body Chern Numbers, Phys. Rev. X **10**, 031008 (2020).
[20] Y. Yao and M. Oshikawa, Twisted Boundary Condition and Lieb-Schultz-Mattis Ingappability for Discrete Symmetries, Phys. Rev. Lett. **126**, 217201 (2021).
[21] Y. Yao, M. Oshikawa, and A. Furusaki, Gappability Index for Quantum Many-Body Systems, Phys. Rev. Lett. **129**, 017204 (2022).
[22] Y. Yao and A. Furusaki, Geometric approach to Lieb-Schultz-Mattis theorem without translation symmetry under inversion or rotation symmetry, Phys. Rev. B **106**, 045125 (2022).
[23] Y. Tada, Lieb-Schultz-Mattis Theorem in Higher Dimensions from Approximate Magnetic Translation Symmetry, Phys. Rev. Lett. **127**, 237204 (2021).
[24] S. A. Parameswaran, A. M. Turner, D. P. Arovas, and A. Vishwanath, Topological order and absence of band insulators at integer filling in non-symmorphic crystals, Nat. Phys. **9**, 299 (2013).
[25] H. Watanabe, H. C. Po, A. Vishwanath, and M. Zaletel, Filling constraints for spin-orbit coupled insulators in symmorphic and nonsymmorphic crystals, Proc. Nat. Acad. Sci. **112**, 14551 (2015).
[26] H. Watanabe, Lieb-Schultz-Mattis-type filling constraints in the 1651 magnetic space groups, Phys. Rev. B **97**, 165117 (2018).
[27] H. C. Po, H. Watanabe, C.-M. Jian, and M. P. Zaletel, Lattice Homotopy Constraints on Phases of Quantum Magnets, Phys. Rev. Lett. **119**, 127202 (2017).
[28] Y. Yao, L. Li, M. Oshikawa, and C.-T. Hsieh, Lieb-Schultz-Mattis theorem for 1d quantum magnets with antiunitary translation and inversion symmetries, arXiv:2307.09843.
[29] Y.-M. Lu, Y. Ran, and M. Oshikawa, Filling-enforced constraint on the quantized Hall conductivity on a periodic lattice, Ann. Phys. **413**, 168060 (2020).
[30] H.-B. Braun and D. Loss, Berry's phase and quantum dynamics of ferromagnetic solitons, Phys. Rev. B **53**, 3237 (1996).
[31] H.-B. Braun and D. Loss, Chiral quantum spin solitons, J. Appl. Phys. **79**, 6107 (1996).
[32] S. Kodama, A. Tanaka, and Y. Kato, Spin parity effects in a monoaxial chiral ferromagnetic chain, Phys. Rev. B **107**, 024403 (2023).
[33] R. Takashima, H. Ishizuka, and L. Balents, Quantum skyrmions in two-dimensional chiral magnets, Phys. Rev. B **94**, 134415 (2016).
[34] E. Altman, W. Hofstetter, E. Demler, and M. D. Lukin, Phase diagram of two-component bosons on an optical lattice, New J. Phys. **5**, 113 (2003).
[35] W. C. Chung, J. de Hond, J. Xiang, E. Cruz-Colón, and W. Ketterle, Tunable Single-Ion Anisotropy in Spin-1 Models Realized with Ultracold Atoms, Phys. Rev. Lett. **126**, 163203 (2021).
[36] J. de Hond, J. Xiang, W. C. Chung, E. Cruz-Colón, W. Chen, W. C. Burton, C. J. Kennedy, and W. Ketterle, Preparation of the Spin-Mott State: A Spinful Mott Insulator of Repulsively Bound Pairs, Phys. Rev. Lett. **128**, 093401 (2022).
[37] F. D. M. Haldane, 'Luttinger liquid theory' of one-dimensional quantum fluids. I. Properties of the Luttinger model and their extension to the general 1D interacting spinless Fermi gas, J. Phys. C: Solid State Phys. **14**, 2585 (1981).
[38] P. Weinberg and M. Bukov, QuSpin: a Python package for dynamics and exact diagonalisation of quantum many body systems part I: spin chains, SciPost Phys. **2**, 003 (2017).
[39] P. Weinberg and M. Bukov, QuSpin: a Python package for dynamics and exact diagonalisation of quantum many body systems. Part II: bosons, fermions and higher spins, SciPost Phys. **7**, 020 (2019).
[40] The source code used for exact diagonalization is available in https://github.com/shuntarosumita/antiferro_spin_parity/tree/main/ed.
[41] See Supplemental Materials, which include Refs. [42–62].
[42] A. G. Catalano, D. Brtan, F. Franchini, and S. M. Giampaolo, Simulating continuous symmetry models with discrete ones, Phys. Rev. B **106**, 125145 (2022).
[43] U. Schollwöck and T. Jolicœur, Haldane Gap and Hidden Order in the $S = 2$ Antiferromagnetic Quantum Spin Chain, Europhys. Lett. **30**, 493 (1995).
[44] T. Tonegawa, K. Okamoto, H. Nakano, T. Sakai, K. Nomura, and M. Kaburagi, Haldane, Large-D, and Intermediate-D States in an $S = 2$ Quantum Spin Chain with On-Site and XXZ Anisotropies, J. Phys. Soc. Jpn. **80**, 043001 (2011).
[45] J. Kurmann, H. Thomas, and G. Müller, Antiferromagnetic long-range order in the anisotropic quantum spin chain, Physica A **112**, 235 (1982).
[46] G. Müller and R. E. Shrock, Implications of direct-product ground states in the one-dimensional quantum XYZ and XY spin chains, Phys. Rev. B **32**, 5845 (1985).
[47] D. V. Dmitriev, V. Y. Krivnov, A. A. Ovchinnikov, and A. Langari, One-dimensional anisotropic Heisenberg model in the transverse magnetic field, J. Exp. Theor. Phys. **95**, 538 (2002).
[48] M. Fishman, S. R. White, and E. M. Stoudenmire, The ITensor Software Library for Tensor Network Calculations, SciPost Phys. Codebases , 4 (2022).
[49] M. Fishman, S. R. White, and E. M. Stoudenmire, Codebase release 0.3 for ITensor, SciPost Phys. Codebases , 4_r0.3 (2022).
[50] F. Pollmann, A. M. Turner, E. Berg, and M. Oshikawa, Entanglement spectrum of a topological phase in one dimension, Phys. Rev. B **81**, 064439 (2010).
[51] L. Gioia and C. Wang, Nonzero Momentum Requires Long-

Range Entanglement, Phys. Rev. X **12**, 031007 (2022).
[52] A. Tanaka, K. Totsuka, and X. Hu, Geometric phases and the magnetization process in quantum antiferromagnets, Phys. Rev. B **79**, 064412 (2009).
[53] E. Fradkin, *Field Theories of Condensed Matter Physics*, 2nd ed. (Cambridge University Press, 2013).
[54] T. T. Wu and C. N. Yang, Dirac monopole without strings: Monopole harmonics, Nucl. Phys. B **107**, 365 (1976).
[55] S. Takayoshi, K. Totsuka, and A. Tanaka, Symmetry-protected topological order in magnetization plateau states of quantum spin chains, Phys. Rev. B **91**, 155136 (2015).
[56] F. D. M. Haldane, O(3) Nonlinear σ Model and the Topological Distinction between Integer- and Half-Integer-Spin Antiferromagnets in Two Dimensions, Phys. Rev. Lett. **61**, 1029 (1988).
[57] S. Sachdev and K. Park, Ground states of quantum antiferromagnets in two dimensions, Ann. Phys. **298**, 58 (2002).
[58] I. Affleck, Mass generation by merons in quantum spin chains and the O(3) σ model, Phys. Rev. Lett. **56**, 408 (1986).
[59] Z.-C. Gu and X.-G. Wen, Tensor-entanglement-filtering renormalization approach and symmetry-protected topological order, Phys. Rev. B **80**, 155131 (2009).
[60] Y. Fuji, F. Pollmann, and M. Oshikawa, Distinct Trivial Phases Protected by a Point-Group Symmetry in Quantum Spin Chains, Phys. Rev. Lett. **114**, 177204 (2015).
[61] S. Sachdev, *Quantum Phases of Matter* (Cambridge University Press, 2023).
[62] X.-G. Wen, *Quantum Field Theory of Many-Body Systems* (Oxford University Press, 2004).
[63] J. B. Parkinson and J. C. Bonner, Spin chains in a field: Crossover from quantum to classical behavior, Phys. Rev. B **32**, 4703 (1985).
[64] M. Takahashi and T. Sakai, Magnetization Curve and Correlation Function of Haldane-Gap Antiferromagnet in Strong Magnetic Field, J. Phys. Soc. Jpn. **60**, 760 (1991).
[65] D. C. Cabra, A. Honecker, and P. Pujol, Magnetization Curves of Antiferromagnetic Heisenberg Spin-$\frac{1}{2}$ Ladders, Phys. Rev. Lett. **79**, 5126 (1997).
[66] M. Arlego, D. C. Cabra, J. E. Drut, and M. D. Grynberg, Competing interactions in the XYZ model, Phys. Rev. B **67**, 144426 (2003).
[67] P. Jordan and E. Wigner, Über das Paulische Äquivalenzverbot, Z. Phys. **47**, 631 (1928).
[68] T. Giamarchi, *Quantum Physics in One Dimension* (Oxford University Press, 2003).
[69] N. Kawakami and S.-K. Yang, Conformal Field Theory Approach to One-Dimensional Quantum Liquids, Prog. Theor. Phys. Suppl. **107**, 59 (1992).
[70] F. D. M. Haldane, Effective Harmonic-Fluid Approach to Low-Energy Properties of One-Dimensional Quantum Fluids, Phys. Rev. Lett. **47**, 1840 (1981); Effective Harmonic-Fluid Approach to Low-Energy Properties of One-Dimensional Quantum Fluids, Phys. Rev. Lett. **48**, 569(E) (1982) (erratum).
[71] R. M. Konik and P. Fendley, Haldane-gapped spin chains as Luttinger liquids: Correlation functions at finite field, Phys. Rev. B **66**, 144416 (2002).
[72] O. Perron, Zur Theorie der Matrices, Math. Ann. **64**, 248 (1907).
[73] G. Frobenius, Über Matrizen aus nicht negativen Elementen, in *Sitzungsberichte der Königlich Preussischen Akademie der Wissenschaften* (1912) p. 456.
[74] In Ref. [7] this observation was applied to the magnetization plateau problem for a $S = 3/2$ spin chain in a longitudinal magnetic field.
[75] H. J. Schulz, Phase diagrams and correlation exponents for quantum spin chains of arbitrary spin quantum number, Phys. Rev. B **34**, 6372 (1986).
[76] M. den Nijs and K. Rommelse, Preroughening transitions in crystal surfaces and valence-bond phases in quantum spin chains, Phys. Rev. B **40**, 4709 (1989).
[77] W. Chen, K. Hida, and B. C. Sanctuary, Ground-state phase diagram of $S = 1$ XXZ chains with uniaxial single-ion-type anisotropy, Phys. Rev. B **67**, 104401 (2003).
[78] F. Pollmann, E. Berg, A. M. Turner, and M. Oshikawa, Symmetry protection of topological phases in one-dimensional quantum spin systems, Phys. Rev. B **85**, 075125 (2012).
[79] J.-H. Huang, G.-M. Zhang, and D.-X. Yao, Dynamical spin excitations of the topological Haldane gapped phase in the $S = 1$ Heisenberg antiferromagnetic chain with single-ion anisotropy, Phys. Rev. B **103**, 024403 (2021).
[80] C. K. Majumdar and D. K. Ghosh, On Next-Nearest-Neighbor Interaction in Linear Chain. I, J. Math. Phys. **10**, 1388 (1969).
[81] F. D. M. Haldane, Spontaneous dimerization in the $S = \frac{1}{2}$ Heisenberg antiferromagnetic chain with competing interactions, Phys. Rev. B **25**, 4925 (1982); Spontaneous dimerization in the $S = \frac{1}{2}$ Heisenberg antiferromagnetic chain with competing interactions, Phys. Rev. B **26**, 5257(E) (1982) (erratum).
[82] N. Read and S. Sachdev, Valence-bond and spin-Peierls ground states of low-dimensional quantum antiferromagnets, Phys. Rev. Lett. **62**, 1694 (1989).
[83] N. Read and S. Sachdev, Spin-Peierls, valence-bond solid, and Néel ground states of low-dimensional quantum antiferromagnets, Phys. Rev. B **42**, 4568 (1990).
[84] S. Sachdev and K. Park, Ground States of Quantum Antiferromagnets in Two Dimensions, Ann. Phys. **298**, 58 (2002).
[85] S. Braun, J. P. Ronzheimer, M. Schreiber, S. S. Hodgman, T. Rom, I. Bloch, and U. Schneider, Negative Absolute Temperature for Motional Degrees of Freedom, Science **339**, 52 (2013).
[86] C. Chen, G. Bornet, M. Bintz, G. Emperauger, L. Leclerc, V. S. Liu, P. Scholl, D. Barredo, J. Hauschild, S. Chatterjee, M. Schuler, A. M. Läuchli, M. P. Zaletel, T. Lahaye, N. Y. Yao, and A. Browaeys, Continuous symmetry breaking in a two-dimensional Rydberg array, Nature **616**, 691–695 (2023).
[87] K. Tsuruta, M. Mito, Y. Kousaka, J. Akimitsu, J.-i. Kishine, Y. Togawa, H. Ohsumi, and K. Inoue, Discrete Change in Magnetization by Chiral Soliton Lattice Formation in the Chiral Magnet $Cr_{1/3}NbS_2$, J. Phys. Soc. Jpn. **85**, 013707 (2016).